Assessment of the Carbon Mineralization Potential of British Columbia by Quantifying the Response of Physical Properties to the Alteration of Ultramafic Rocks (NTS 092H/08, 10, 093K/13, 14, 094C/05, 104I, 104N)

J.A. Cutts, Bradshaw Research Initiative for Minerals and Mining, The University of British Columbia, Vancouver, British Columbia, jcutts@eoas.ubc.ca

G.M. Dipple, Bradshaw Research Initiative for Minerals and Mining, The University of British Columbia, Vancouver, British Columbia

C.J.R. Hart, Mineral Deposits Research Unit, The University of British Columbia, Vancouver, British Columbia

D. Milidragovic, British Columbia Geological Survey, Ministry of Energy, Mines and Petroleum Resources, Victoria, British Columbia

Cutts, J.A., Dipple, G.M., Hart, C.J.R. and Milidragovic, D. (2020): Assessment of the carbon mineralization potential of British Columbia by quantifying the response of physical properties to the alteration of ultramafic rocks (NTS 092H/08, 10, 093K/13, 14, 094C/05, 104I/01–16, 104N/01–16); *in* Geoscience BC Summary of Activities 2019: Minerals, Geoscience BC, Report 2020-01, p. 137–144.

Introduction

British Columbia (BC) contains large volumes of ultramafic rocks (Figure 1) and these have been, and continue to be, of economic interest due to the common occurrence of Ni±Fe-Cu-PGE mineralization (e.g., Nixon et al., 2015; Britten, 2017). However, resource extraction typically produces large volumes of solid waste and contributes significant carbon dioxide (CO_2) emissions, presenting both an environmental and—given BC's and Canada's carbon tax—an economic challenge. Recent research has demonstrated the potential of ultramafic rocks and their serpentinized products to react with and sequester CO_2 (e.g., Hansen et al., 2005; Keleman and Matter, 2008; Wilson et al., 2009). As such, BC's carbon offset scheme provides companies mining ultramafic rocks with significant economic incentive for reacting mine tailings with either atmospheric or emission-related CO_2. The alteration of ultramafic rocks (Figure 2) can be broadly divided into two main stages: 1) serpentinization, which involves the hydration of Mg-rich silicate minerals, and 2) carbonation, which involves the reaction of serpentinization-related minerals with CO_2 and the formation of Mg-carbonate and -silicate minerals and quartz into a rock termed listwanite (e.g., Kelemen and Hirth, 2012; Power et al., 2013). Strongly serpentinized rocks represent the primary target for carbon sequestration, which occurs through naturally occurring carbonation reactions (e.g., Hansen et al., 2005).

Ultramafic rocks in BC are mainly exposed along a province-wide south-southeast-trending belt (Figure 1). The first-order distribution of these rocks is known and, locally mapped in detail; however, this is not true for all occurrences in the province and, more importantly, the degree of serpentinization and carbonation in all cases is poorly constrained. As such, the potential of these rocks for carbon sequestration remains uncertain. Due to the time investment required to map, sample, and analyze the geochemistry of every occurrence in detail, it is of great interest to develop remote sensing techniques that can identify and quantify the degree to which the ultramafic rocks are serpentinized or carbonated and, thus, their potential to be used as carbon sinks.

The serpentinization of ultramafic rocks (reaction 1 (R1) in Figure 2) mainly involves the hydration and breakdown of the constituents olivine [$(Mg,Fe)_2SiO_4$] and orthopyroxene [$(Mg,Fe)SiO_3$] (e.g., Toft et al., 1990). During serpentinization, Mg^{2+} (and to a lesser extent Fe^{2+}) is incorporated into serpentine-group minerals [$(Mg, Fe)_3(Si_2O_5)(OH)_4$] and brucite [$(Mg,Fe)(OH)_2$], while some Fe^{2+} is oxidized to Fe^{3+} and incorporated into magnetite (Fe_3O_4; Kelemen and Hirth, 2012). Locally, Fe^{2+} may be reduced to Fe^0 and incorporated into awaruite (Ni_3Fe or Ni_2Fe; e.g., Britten, 2017). The hydration process is associated with 25–50% volume increase (Schwarzenbach, 2016) and, in doing so, the rocks may incorporate as much as 15–16 wt. % H_2O (Komor et al., 1985). Brucite has been shown to be highly reactive with CO_2—even at room temperature—and, thus, is the primary targeted mineral for low-cost carbon sequestration (e.g., Vanderzee et al., 2018, 2019); serpentine-group minerals are far less reactive (e.g., Daval et al., 2013). The highest brucite contents are predicted to result from the serpentinization of the most olivine-rich (Si-poor) ultramafic rocks and should be associated with high degrees of hydration. Due to the net volume increase associated with the ser-

This publication is also available, free of charge, as colour digital files in Adobe Acrobat® PDF format from the Geoscience BC website: http://www.geosciencebc.com/updates/summary-of-activities/.

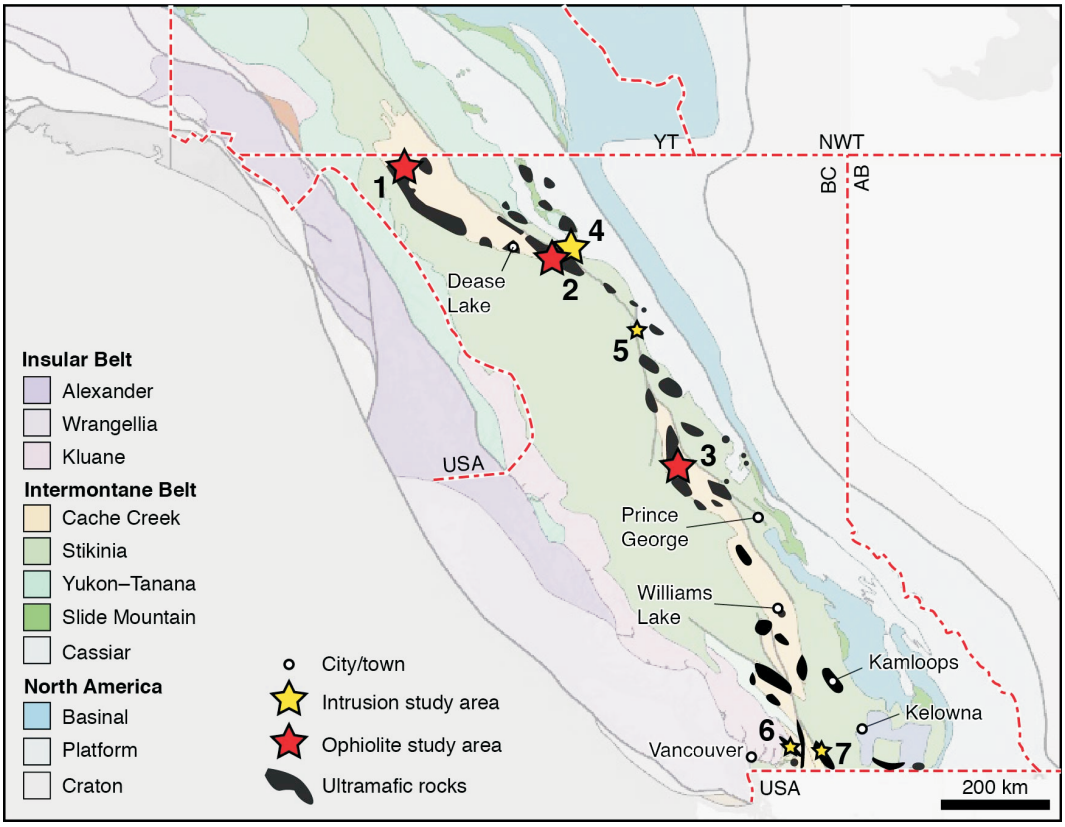

Figure 1. Tectonostratigraphic map of British Columbia showing the distribution of ultramafic rocks and the study areas of interest for this research. Ophiolite-hosted ultramafic study areas include Atlin (1), King Mountain (2) and Decar (3), while intrusion-hosted ultramafic study areas include Turnagain (4), Polaris (5), Giant Mascot (6) and Tulameen (7). Study sites 1–4 (large stars) will serve as the primary study sites for developing petrological and physical rock property models, whereas study sites 5–7 (small stars) will serve as secondary study sites. (Map modified from Cui et al., 2017).

pentinization reactions and due to the production of magnetite, brucite-rich rocks should be distinguished from less serpentinized rocks by being less dense and more magnetic (Toft et al., 1990). The progressive carbonation of serpentinized ultramafic rocks (Figure 2) is subdivided into three stages: reaction 2 (R2) involves the formation of (ferro-)magnesite [$(Mg,Fe)CO_3$] and the continued formation of serpentine-group minerals at the expense of olivine or brucite; reaction 3 (R3) involves the breakdown of serpentine-group minerals and magnetite and the reduction of Fe^{3+} to Fe^{2+} to form (ferro-)magnesite and talc-minnesotaite [$(Mg,Fe)_3Si_4O_{10}(OH_2)$]; and reaction 4 (R4) involves the formation of magnesite and quartz (SiO_2) at the expense of talc-minnesotaite (Forbes, 1971; Hansen et al., 2005). The first two stages of carbonation are associated with a net loss of H_2O and gain of CO_2, whereas during the final stage, H_2O is no longer present and thus, it is associated with only a gain of CO_2. The latter two reactions should result in rocks that are denser and less magnetic.

The response of various physical rock properties of ultramafic rocks, such as magnetic susceptibility and density, to serpentinization and carbonation have been investigated previously (e.g., Toft et al., 1990; Hansen, 2005; Hansen et al., 2005); however, quantitative estimates of these relationships have not been systematically tested in multiple ultramafic rock localities, or have been focused on the carbonation process only. The serpentinization process is particularly important as it results in the formation of the primary carbon sequestration targets, serpentinites. Still, characterization of the carbonation process is important to identify rocks that are not suitable for sequestration purposes. This research aims to identify and quantify the relationship between the alteration of ultramafic rocks and physical rock properties in four key localities in BC (Figure 1) for which detailed mapping and geochemical studies have already been completed. A key question that will be addressed is whether or not these relationships are uniform or vary among the localities. The relationships established between alteration and physical rock properties from these study areas will then be used to inform geophysical inversions that will be used to build 3-D models for carbon sequestration in each site, and will be applied to the other ultramafic rock occurrences (see Figure 1) to establish a carbon sequestration potential index for BC. This paper presents preliminary results for initial work conducted from July 2019 to September 2019.

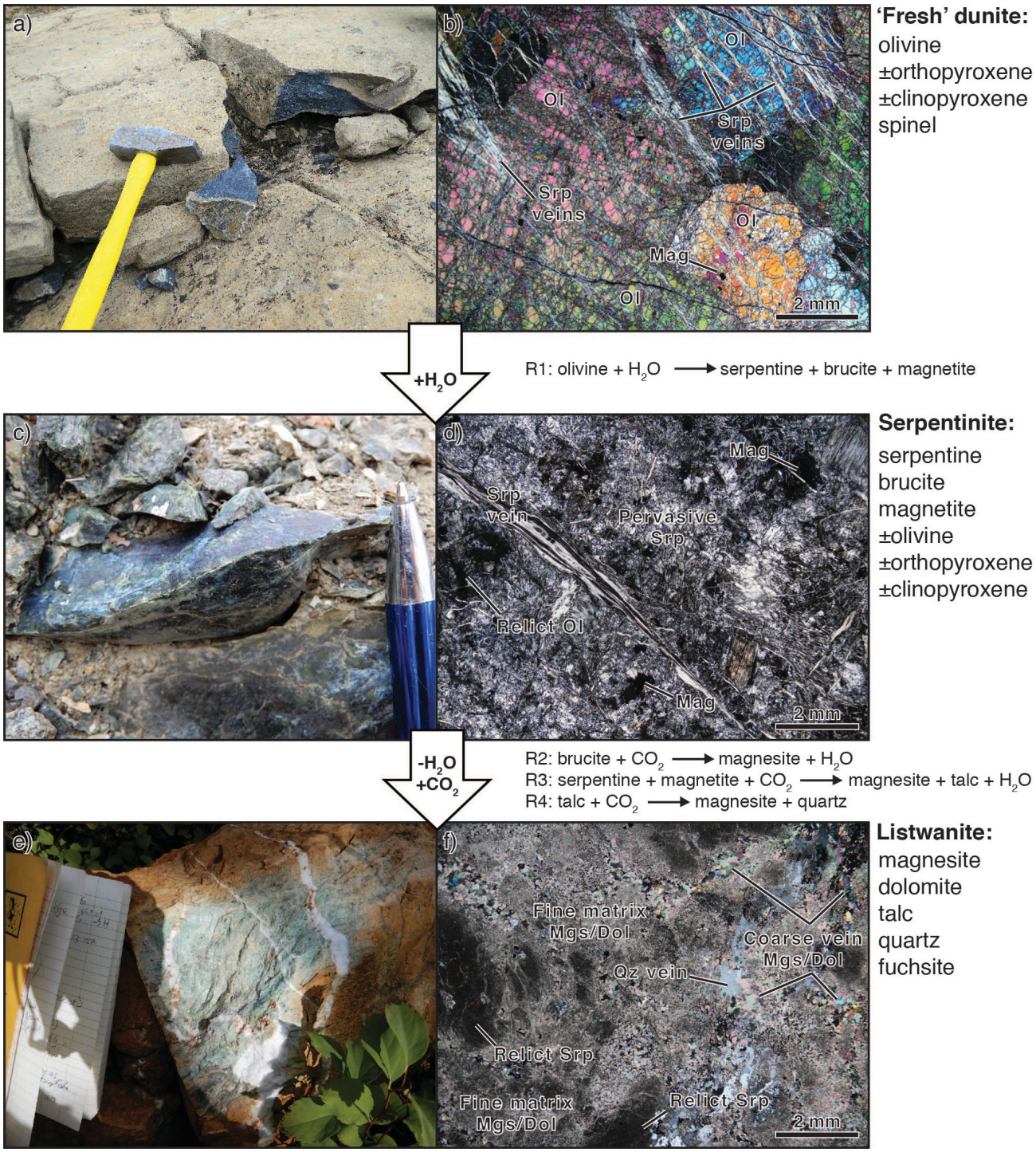

Figure 2. Photographs (a, c, e) and photomicrographs taken in crossed-polarized light (b, d, f) of representative samples from the Decar area. **a, b)** Relatively fresh (~30% serpentine) dunite that comprises coarse olivine (Ol), disseminated magnetite (Mag) and trace spinel, all of which are cut by veinlets of serpentine (Srp). **c, d)** Serpentinite (90–100% serpentine) showing a pervasively serpentinized matrix with globular to blebby magnetite (Mag) and preserved relict olivine (Ol), all of which are crosscut by a vein of serpentine (Srp). **e, f)** Listwanite that comprises magnesite (Mgs), dolomite (Dol), quartz (Qz), fuchsite and talc (fuchsite and talc not shown in the photomicrograph). R1, 2, 3 and 4 are reactions (see text for more details).

Study Localities

The ultramafic rocks of interest occur in two main associations: as ophiolite massifs (e.g., Schiarizza and MacIntyre, 1999; Zagorevski et al., 2017), or as intrusive complexes (e.g., Nixon et al., 2015). The four main localities selected for this study are the Decar, Atlin and King Mountain areas, which are ophiolitic ultramafic massifs, and the Turnagain Alaskan-type intrusion. Three additional intrusions (Polaris, Giant Mascot, Tulameen) may be investigated; however, these are secondary study sites. The Decar area is one of the main localities of ongoing research (e.g., Vanderzee et al., 2018, 2019) at the Bradshaw Research Initiative for Minerals and Mining (BRIMM) at the Department of Earth, Ocean and Atmospheric Sciences (EOAS), University of British Columbia (UBC), and is in collaboration with the Mineral Deposits Research Unit (MDRU) at UBC, FPX Nickel, and the British Columbia Geological Survey (BCGS). The area has been mapped in detail and the geochemistry of the rocks has been studied by the BCGS (Milidragovic et al., 2018; Milidragovic, 2019; Milidragovic and Grundy, 2019) and FPX Nickel (e.g., Britten, 2017); however, these studies were focused on regional-scale correlations among all rock types, or were focused only on the highly serpentinized and mineralized rocks. Two weeks of additional fieldwork in summer 2019 by researchers at BRIMM resulted in a comprehensive sample suite spanning the full range of serpentinized and carbonated ultramafic rock types, and these will complement the existing samples and datasets (Table 1).

The ultramafic rocks in and immediately surrounding the town of Atlin have been the subject of several graduate student theses at EOAS (e.g., Hansen, 2005) and the surrounding area has been one of the main foci of the Geological Survey of Canada's (GSC) Geo-mapping for Energy and Minerals, Phase 2 (GEM-2) research program (e.g., Zagorevski et al., 2017). The Atlin area ultramafic rocks are subdivided into two main areas: 1) the Atlin ophiolite (e.g., Hansen et al., 2005; Zagorevski et al., 2017), and 2) the Nahlin ophiolite (e.g., McGoldrick et al., 2017, 2018; Zagorevski et al., 2017). The extensive sample suites and whole-rock geochemistry results from the EOAS theses and from GEM-2 have been made available for this study (Table 1). The King Mountain area has not been sampled as extensively as the other two ophiolitic areas; however, it was studied as part of GEM-2 and the sample suite and whole-rock geochemistry results have been made available for this study (Table 1). Additionally, the King Mountain area was at one point considered by FPX Nickel as a target for Fe-Ni exploration (e.g., Letain locality in Britten, 2017).

The Turnagain Alaskan-type mafic-ultramafic intrusion (e.g., Nixon et al., 2015) has been the subject of several graduate theses at UBC (e.g., Scheel, 2007; Jackson-Brown, 2017) and has been extensively studied by Giga Metals Corp. as one of the largest undeveloped Ni-Cu-PGE deposits in the province. BRIMM has recently entered into a research partnership with Giga Metals; the number and

Table 1. Summary of the localities of interest for this study, and the status of progress into the whole-rock chemical analyses and physical property measurements. For sample suites with finished datasets, the numbers in columns indicate the number of samples analyzed; 'In progress' refers to sample suites for which analyses have begun but are not yet complete; 'TBD' (to be determined) refers to sample suites for which analyses have not yet begun.

Locality	Ophiolite	Locality details	Source	Whole-rock chemistry	CO_2 content	Magnetic Susceptibility[1]	Density[1]
Atlin Area	Atlin	Atlin (town)	Hansen (2005)	160	160	116	In progress
		Atlin (town)	Zagorevski (2018)	26	TBD	In progress	In progress
		Mount Barham	Zagorevski (2018)	12	TBD	In progress	In progress
		Sentinal Peak	Zagorevski (2018)	7	TBD	In progress	In progress
		Union Mountain	Zagorevski (2018)	22	TBD	In progress	In progress
	Nahlin	Menatutuline Peak	Zagorevski (2018)	58	TBD	In progress	In progress
		Mount Nimbus	Zagorevski (2018)	5	TBD	In progress	In progress
		Mount O'Keefe/Focus	Zagorevski (2016, 2018)	5	TBD	In progress	In progress
		Nahlin Mountain	Zagorevski (2018)	7	TBD	In progress	In progress
		Peridotite Peak	Zagorevski (2018)	7	TBD	In progress	In progress
Decar Area	Decar	Baptiste deposit	BRIMM	In progress	TBD	17	In progress
			Milidragovic and Grundy (2019)	1	TBD	9	In progress
			FPX Nickel	18	18	8	In progress
		Van deposit	BRIMM	In progress	TBD	6	In progress
			Milidragovic and Grundy (2019)	6	TBD	17	In progress
		Mount Sydney-Williams	BRIMM	In progress	TBD	20	In progress
			Milidragovic and Grundy (2019)	3	TBD	5	In progress
		Other	BRIMM	In progress	TBD	23	In progress
			Milidragovic and Grundy (2019)	2	TBD	22	In progress
King Mountain Area	Unnamed	King Mountain	Zagorevski (2016, 2018)	26	TBD	In progress	In progress
Turnagain Intrusion	-	-	Jackson-Brown (2017)	17	-	-	-
Polaris Intrusion	-	-	-	-	-	-	-
Giant Mascot Intrusion	-	-	-	-	-	-	-
Tullameen Intrusion	-	-	-	-	-	-	-

[1]Measured on hand samples at UBC

nature of the samples that will be made available for study are, as yet, uncertain.

Methods

Whole-Rock Geochemistry

Whole-rock major-element geochemistry—compiled from the literature and from newly collected samples—will be used to characterize and calculate the composition and mineralogy of the protolith and the extent of alteration of the samples (Table 1). Specifically, the calculated olivine/pyroxene content of the protolith will be used to predict the brucite potential, and the H_2O and CO_2 contents of the rocks will be important to determine the degree to which the samples have been serpentinized and carbonated, respectively. Major-element chemistry results have been or currently are being determined by X-ray fluorescence (XRF) at various commercial laboratories, including Activation Laboratories (Ancaster, Ontario) and ALS Geochemistry (North Vancouver, British Columbia).

Physical Properties

The main physical properties of interest are magnetic susceptibility and density. Magnetic susceptibility was measured using a ZH Instruments SM30 instrument, and sample thickness and demagnetization corrections were applied. Measurements were done in the field primarily on flat, weathered surfaces, whereas measurements done in the lab were done on flat (cut), fresh surfaces; this approach was used to characterize the effects of surface weathering and because fresh surfaces in the field are rare. To capture the intra-sample heterogeneity, each plotted magnetic susceptibility value represents 5–10 individual measurements from various parts of the sample or outcrop; for weathered surfaces, the highest measurements were averaged, whereas for fresh surfaces an average of all measurements was used. This approach was taken because magnetite tends to break down during the weathering of ultramafic rocks and, thus, the highest values should reflect the least altered rock. Sample masses for density determination were measured using an A&D Company Ltd. EJ-6100 balance. Density was calculated using Archimedes principal, which uses the dry and wet masses of the samples and applying equation (1)

$$\rho_s = \rho_w\left[\frac{m_{dry}}{m_{dry}-m_{wet}}\right] \quad , \qquad (1)$$

where ρ_s = density of the sample in g/cm^3, ρ_w = density of water, m_{dry} = mass in air in grams, and m_{wet} = mass in water in grams. This equation is simplified by using a density for water of 1 g/cm^3, which is true at temperatures of 25°C and pressures of 1 bar. To assess the accuracy of our magnetic susceptibility and density measurements, and to provide additional information on the porosity, permeability and electrical conductivity of the sampled ultramafic rocks, a selection of samples will be sent to the Paleomagnetism and Petrophysics Laboratory (PPL) at GSC–Pacific in Sidney, BC. All measurements will be done on a 2.5 cm diameter core of unweathered material using a Sapphire Instruments SI2B instrument to measure magnetic susceptibility, a specially built Jolly balance to determine density, and a Solartron 1260 Frequency Response Analyzer and Gamry Reference 600+ Potentiostat to measure electrical impedance (resistance/conductivity or energy loss in a circuit; Enkin, 2017).

Preliminary Results

Hansen et al. (2005) used a limited set of samples (~20) from a relatively restricted area in the Atlin ophiolite to establish a semiquantitative relationship between the carbonation of serpentinite and magnetic susceptibility. To further explore this relationship, additional samples from the same ophiolite (Hansen, 2005), for which there are corresponding whole-rock geochemistry data, were analyzed for their magnetic susceptibility; density measurements are ongoing. The volatile components of the whole-rock geochemistry (H_2O and CO_2) for the samples and their corresponding magnetic susceptibility are consistent with what is predicted on the basis of the observed mineral assemblages and the reactions that they reflect (Figure 3). As the degree of serpentinization increases, as indicated by increasing H_2O contents up to 13–15 wt. %, so too does the magnetic susceptibility of the rocks; this is consistent with increased production of magnetite during reaction 1 (R1; Figures 2, 3). Pure serpentine-group minerals and brucite can accommodate up to 13 wt. % and 31 wt. % H_2O, respectively (e.g., Komor et al., 1985), thus the observed volatile compositions in the analyzed rocks (with CO_2 <1 wt. %) are consistent with variable mixtures of olivine, serpentine and brucite. Due to a lack of unhydrated samples from the Atlin ophiolite, the response of magnetic susceptibility to low degrees of serpentinization (H_2O <8 wt. %) has yet to be investigated (Figure 3); this will be addressed in future work.

Reaction 2 involves a net loss of H_2O and gain of CO_2 from the system. For samples that have undergone mild carbonation (<5 wt. % CO_2), there is no appreciable decrease in magnetic susceptibility relative to uncarbonated samples (Figure 3), implying that magnetite has not been consumed. Whether or not brucite is still present at this stage is as yet uncertain. Further carbonation of the samples (R3: >5 wt. % CO_2) results in a marked decrease in magnetic susceptibility (Figure 3), which is consistent with magnetite breakdown, the reduction of Fe^{3+} to Fe^{2+}, and the formation of (ferro-)magnesite and talc-minnesotaite. Samples that have undergone the final stage of carbonation (R4) have the lowest associated magnetic susceptibility (Figure 3), consistent with complete breakdown of magnetite.

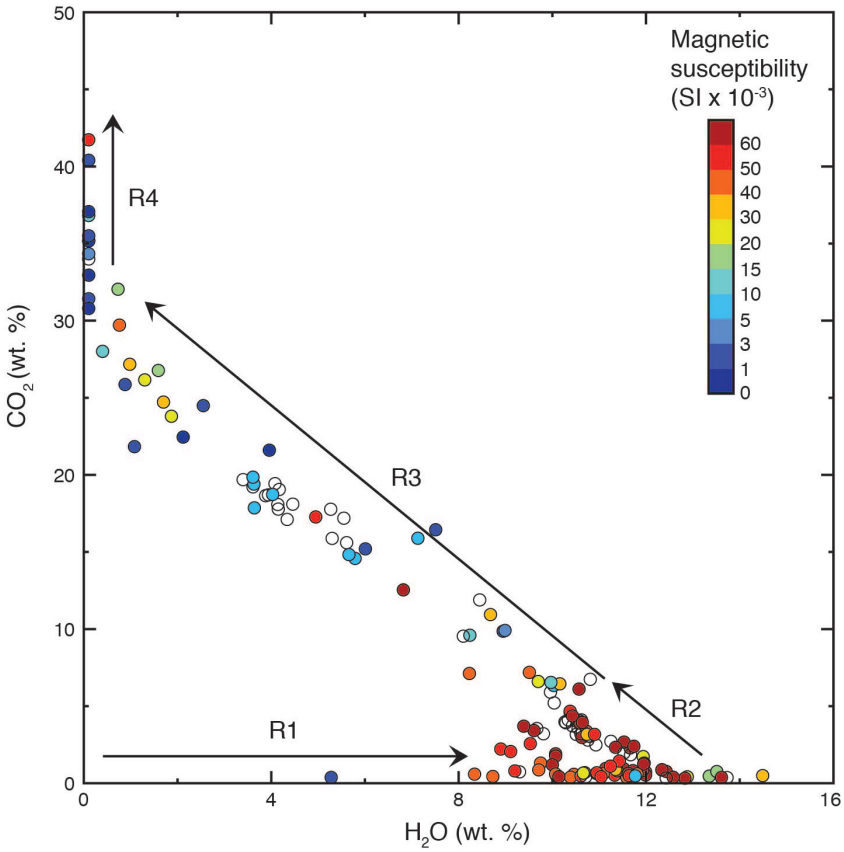

Figure 3. CO_2 and H_2O (loss on ignition – CO_2) concentrations in wt. % of ultramafic samples from the immediate vicinity of the town of Atlin, with colours assigned based on their corresponding magnetic susceptibility; white circles represent samples for which there is no corresponding magnetic susceptibility measurement. Reactions 1 to 4 (R1–R4) refer to the mineral reactions occurring during serpentinization and carbonation that are described in the main text and Figure 2. High degrees of serpentinization, as indicated by H_2O concentrations of 10–14 wt. %, are associated with the highest magnetic susceptibility and likely reflect the formation of magnetite during R1. The initial stage of carbonation (R2) does not result in an appreciable decrease in magnetic susceptibility but may cause the breakdown of brucite (Daval et al., 2013), the main target mineral for carbon sequestration (Vanderzee et al., 2018, 2019). Subsequent carbonation reactions (R3 and R4) result in an overall drop in magnetic susceptibility due to the breakdown of magnetite.

The relationships between H_2O, CO_2 and magnetic susceptibility deduced from the Atlin area samples will serve as a framework to compare results from other ultramafic rock localities. Analysis of the magnetic susceptibility of the Decar area samples (Figure 4) demonstrates—as predicted—that the highest values obtained from weathered surfaces in the field are typically lower than those obtained from the fresh surfaces in the lab (Figure 4a). This first-order observation will be further explored through detailed physical property analysis at the PPL at GSC–Pacific in Sidney. The density of the Decar area samples has been constrained, and shows a broadly negative correlation between density and magnetic susceptibility (Figure 4b), reflecting the net volume–increasing reactions and magnetite production associated with serpentinization; this is consistent with the predicted mineral reactions and with observations made on other, similar, peridotite bodies (e.g., Toft et al., 1990). Once received, the whole-rock chemical analyses of the samples from the Decar area will enable further testing of the established physical property trends.

Conclusions and Future Work

Preliminary analysis of the magnetic susceptibility of a suite of samples from the Atlin ophiolite are consistent with the observed mineral assemblages and the inferred reactions. The observed trends will be used as a framework for future analyses of samples from the Atlin, Decar and King Mountain ophiolites, and the Turnagain Alaskan-type intrusion. Magnetic susceptibility and density measurements of the Decar area samples indicate a negative correlation between the two physical properties; serpentinization is associated with an increase in magnetic susceptibility and decrease in density, whereas carbonation is associated with the opposite trend. These relationships will be further tested using samples from other localities, and these will form the basis for interpreting airborne geophysical sur-

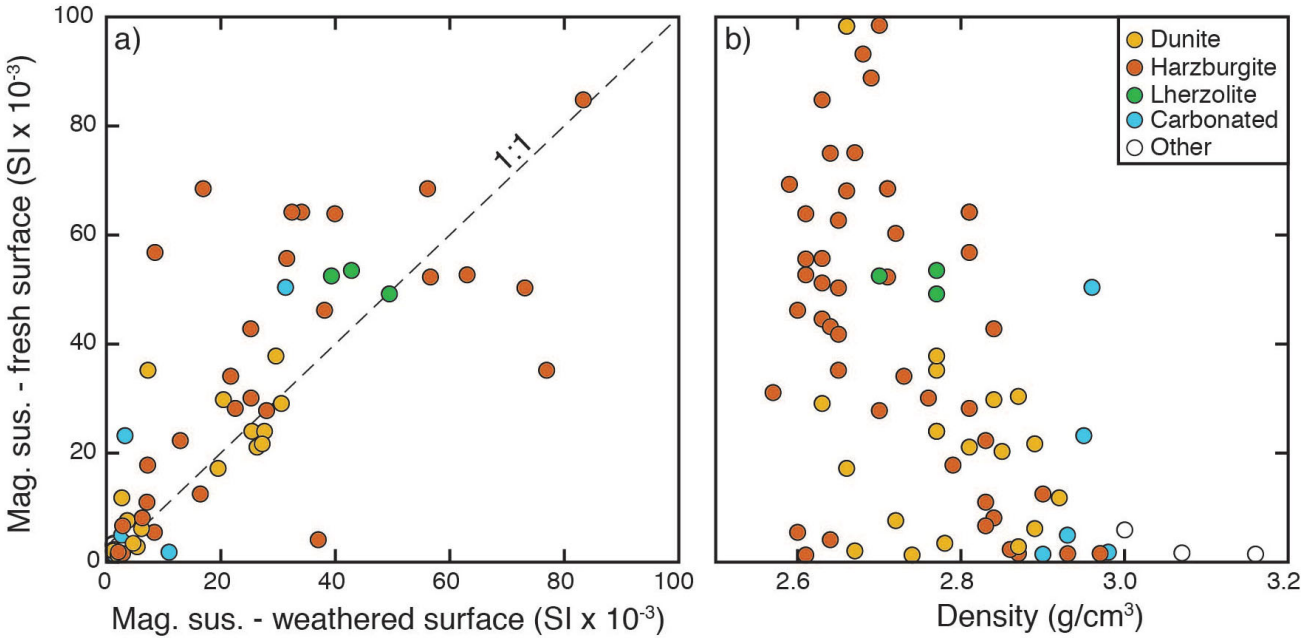

Figure 4. a) Comparison of magnetic susceptibility (Mag. sus.) measurements taken from the weathered surface in the field and on fresh surfaces in the lab for Decar area samples. Field measurements (n = 5–10 per sample) were done on the weathered surface and the plotted value reflects the average of the highest values, whereas lab measurements were done on the fresh surface and the value reflects the average of five measurements. In general, the two datasets fall close to a 1:1 correlation line; however, values tend to be higher for measurements on the fresh surfaces. This discrepancy reflects the propensity for magnetite to break down during weathering. **b)** Comparison of magnetic susceptibility and specific gravity of samples from the Decar area, coloured by rock type as determined using a CIPW normalization scheme. The samples show a broadly negative correlation, with carbonated and non-ultramafic samples ('Other') distinctly less magnetic and denser than the variably serpentinized samples.

veys to evaluate the extent of serpentine and carbonate alteration of ultramafic rocks.

Acknowledgments

In addition to Geoscience BC, the authors thank FPX Nickel Corp., Giga Metals Corp., and the Natural Sciences and Engineering Research Council for financial support of this project. The authors also thank A. Zagorevski at the Geological Survey of Canada–Central Division for providing access to samples from the northern BC ophiolites, which were collected as part of the Geo-mapping for Energy and Minerals, Phase 2 research program. This paper benefited from a constructive review by S. Peacock from The University of British Columbia.

References

Britten, R. (2017): Regional metallogeny and genesis of a new deposit type—disseminated awaruite (Ni_3Fe) mineralization hosted in the Cache Creek Terrane; Economic Geology, v. 112, p. 517–500.

Cui, Y., Miller, D., Schiarizza, P. and Diakow, L.J. (2017): British Columbia digital geology; BC Ministry of Energy, Mines and Petroleum Resources, BC Geological Survey, Open File 2017-8, 9 p. Data version 2018-04-05.

Daval, D., Hellmann, R., Martinez, I., Gangloff, S. and Guyot, F. (2013): Lizardite serpentine dissolution kinetics as a function of pH and temperature, including effects of elevated pCO_2; Chemical Geology, v. 351, p. 245–256.

Enkin, R.J. (2017): Physical property measurements at the Geological Survey of Canada Paleomagnetism and Petrophysics laboratory; Explorations 2017 Petrophysics Workshop, p. 02-1–02-16.

Forbes, W.C. (1971): Iron content of talc in the system $Mg_3Si_4O_{10}(OH)_2$-$Fe_3Si_4O_{10}(OH)_2$; Journal of Geology, v. 79, p. 63–74.

Hansen, L. (2005): Geologic setting of listwanite, Atlin, B.C.: implications for carbon dioxide sequestration and lode-gold mineralization; M.Sc. thesis, The University of British Columbia, Vancouver, BC, 192 p.

Hansen, L.D., Dipple, G.M., Gordon, T.M. and Kellett, D.A. (2005): Carbonated serpentinite (listwanite) at Atlin, British Columbia: a geological analogue to carbon dioxide sequestration; Vancouver Island, Canada; Canadian Mineralogist, v. 43, p. 225–239.

Jackson-Brown, S. (2017): Origin of Cu-PGE-rich sulfide mineralization in the DJ/DB zone of the Turnagain Alaskan-type intrusion, British Columbia; M.Sc. thesis, The University of British Columbia, Vancouver, BC, 272 p.

Kelemen, P.B. and Hirth, G. (2012): Reaction-driven cracking during retrograde metamorphism: olivine hydration and carbonation; Earth and Planetary Science Letters, v. 345–348, p. 81–89.

Kelemen, P.B. and Matter, J. (2008): In situ carbonation of peridotite for CO_2 storage; Proceedings from the National Academy of Science, v. 105, no. 45, p. 17295–17300.

Komor, S.C., Elthon, D. and Casey, J.F. (1985): Serpentinization of cumulate ultramafic rocks from the North Arm Mountain massif of the Bay of Islands ophiolite; Geochimica et Cosmochimica Acta, v. 49, p. 2331–2338.

McGoldrick, S., Canil, D. and Zagorevski, A. (2018): Contrasting thermal and melting histories for segments of mantle lithosphere in the Nahlin ophiolite, British Columbia, Canada; Contributions to Mineralogy and Petrology, v. 173, p. 25–42.

McGoldrick, S., Zagorevski, A. and Canil, D. (2017): Geochemistry of the volcanic and plutonic rocks from the Nahlin ophiolite with implications for a Permo-Triassic arc in the Cache Creek terrane, northwestern British Columbia; Canadian Journal of Earth Sciences, v. 54, p. 1214–1227.

Milidragovic, D. (2019): Geology of the Cache Creek terrane north of Trembleur Lake, parts of NTS 93K/14; BC Ministry of Energy, Mines and Petroleum Resources, BC Geological Survey, Open File 2019-06, 1:50 000 scale.

Milidragovic, D. and Grundy, R. (2019): Geochemistry and petrology of rocks in the Decar area, central British Columbia: Petrologically constrained subdivision of the Cache Creek complex; *in* Geological Fieldwork 2018, BC Ministry of Energy, Mines and Petroleum Resources, BC Geological Survey, Paper 2019-1, p. 55–77.

Milidragovic, D., Grundy, R. and Schiarizza, P. (2018): Geology of the Decar area north of Trembleur Lake; NTS 93K/14; *in* Geological Fieldwork 2017, BC Ministry of Energy, Mines and Petroleum Resources, BC Geological Survey, Paper 2018-1, p. 129–142.

Nixon, G.T., Manor, M.J., Jackson-Brown, S., Scoates, J.S. and Ames, D.E. (2015): Magmatic Ni-Cu-PGE sulphide deposits at convergent margins; *in* Targeted Geoscience Initiative 4: Canadian Nickel-Copper-Platinum Group Elements-Chromium Ore Systems—Fertility, Pathfinders, New and Revised Models, D.E. Ames and M.G. Houlé (ed.), Geological Survey of Canada, Open File 7856, p. 17–34.

Power, I.M., Wilson, S.A. and Dipple, G.M. (2013): Serpentinite carbonation for CO_2 sequestration; Elements, v. 9, p. 115–121.

Scheel, E.J. (2007): Age and origin of the Turnagain Alaskan-type intrusion and associated Ni-sulphide mineralization, north-central British Columbia, Canada; M.Sc. thesis, The University of British Columbia, Vancouver, BC, 201 p.

Schiarizza, P. and MacIntyre, D. (1999): Geology of the Babine Lake–Takla Lake area, central British Columbia (93K/11, 12, 13, 14; 93N/3, 4, 5, 6); *in* Geological Fieldwork 1998, BC Ministry of Energy, Mines and Petroleum Resources, BC Geological Survey, Paper 1999-1, p. 33–68.

Schwarzenbach, E.M. (2016): Serpentinization and the formation of fluid pathways; Geology, v. 44, no. 2, p. 175–176.

Toft, P.B., Arkani-Hamed, J. and Haggerty, S.E. (1990): The effects of serpentinization on density and magnetic susceptibility: a petrological model; Physics of the Earth and Planetary Interiors, v. 65, p. 137–157.

Vanderzee, S.S.S., Dipple, G.M. and Bradshaw, P.M.D. (2019): Targeting highly reactive labile magnesium in ultramafic tailings for greenhouse-gas offsets and potential tailings stabilization at the Baptiste deposit, central British Columbia (NTS 093K/13, 14); *in* Geoscience BC Summary of Activities 2018: Minerals and Mining, Geoscience BC, Report 2019-01, p. 109–118, URL <http://cdn.geosciencebc.com/pdf/SummaryofActivities2018/MM/Schol_SoA2018_MM_Vanderzee.pdf> [November 2019].

Vanderzee, S.S.S., Power, I.M., Dipple, G.M. and Bradshaw, P.M.D. (2018): Carbon mineralization in ultramafic tailings, central British Columbia: a prospect for stabilizing mine waste and reducing greenhouse gas emissions; *in* Geoscience BC Summary of Activities 2017: Minerals and Mining, Geoscience BC, Report 2018-01, p. 109–112, URL <http://cdn.geosciencebc.com/pdf/SummaryofActivities2017/MM/SoA2017_MM_Vanderzee.pdf> [November 2019].

Wilson, S.A., Dipple, G.M., Power, I.M., Thom, J.M., Anderson, R.G., Raudsepp, M., Gabites, J.E. and Southam, G. (2009): Carbon dioxide fixation within mine wastes of ultramafic-mafic-hosted ore deposits: Examples from the Clinton Creek and Cassiar chrysotile deposits, Canada; Economic Geology, v. 104, p. 95–112.

Zagorevksi, A. (2016): Geochemical data of the northern Cache Creek and Stikine terranes and their overlap assemblages, British Columbia and Yukon; Geological Survey of Canada, Open File 8039, 13 p.

Zagorevksi, A. (2018): Geochemical data of the northern Cache Creek, Slide Mountain, and Stikine terranes and their overlap assemblages, British Columbia and Yukon; Geological Survey of Canada, Open File 8395, 12 p.

Zagorevski, A., Bédard, J.H., Bogatu, A., Coleman, M., Golding, M. and Joyce, N. (2017): Stikinia bedrock report of activities, British Columbia and Yukon: GEM2 Cordillera; Geological Survey of Canada, Open File 8329, 13 p.